OPEN

Rat Sciatic Nerve Reconstruction Across a 30 mm Defect Bridged by an Oriented Porous PHBV Tube With Schwann Cell as Artificial Nerve Graft

Mina Karimi,* Esmaeil Biazar,† Saeed Heidari Keshel,* Abdolaziz Ronaghi,‡
Jafar Doostmohamadpour,‡ Alireza Janfada,§ and Arash Montazeri†

An oriented poly(3-hydroxybutyrate-co-3-hydroxyvalerate) nerve conduit has been used to evaluate its efficiency based on the promotion of peripheral nerve regeneration in rats. The oriented porous micropatterned artificial nerve conduit was designed onto the micropatterned silicon wafers, and then their surfaces were modified with oxygen plasma to increase cell adhesion. The designed conduits were investigated by cell culture analyses with Schwann cells (SCs). The conduits were implanted into a 30 mm gap in sciatic nerves of rats. Four months after surgery, the regenerated nerves were monitored and evaluated by macroscopic assessments and histology and behavioral analyses. Results of cellular analyses showed suitable properties of designed conduit for nerve regeneration. The results demonstrated that in the polymeric graft with SCs, the rat sciatic nerve trunk had been reconstructed with restoration of nerve continuity and formatted nerve fibers with myelination. Histological results demonstrated the presence of Schwann and glial cells in regenerated nerves. Functional recovery such as walking, swimming, and recovery of nociceptive function was illustrated for all the grafts especially conduits with SCs. This study proves the feasibility of the artificial nerve graft filled with SCs for peripheral nerve regeneration by bridging a longer defect in an animal model. *ASAIO Journal* 2014; 60:224–233.

Key Words: sciatic regeneration, Schwann cell, artificial conduit, oriented PHBV, histological and behavioral assessments

Following peripheral nerve injury, axons are unable to bridge the gap between damaged nerve stumps.[1] The regenerative environment, including adhesion molecules, growth factors, and Schwann cells (SCs), necessary to promote axonal growth can only support axonal extension for a few millimeters.[1–3] A nerve injury can interfere with communication between the brain and the muscles controlled by a nerve, affecting a person's ability to move certain muscles or have normal sensations.[4] Nerve guides can be made of biological or synthetic materials, and among the latter, both nonabsorbable (*e.g.*, silicon) and biodegradable tubes have been used. Biodegradable nerve guides must be preferred because no foreign body material will be left in the host after the device has fulfilled its task.[5–14] Nerve guides have been fabricated from a variety of materials including gelatin,[15] hyaluron,[16] lactosorb,[17] fibronectin,[18] and polycaprolactone.[19] Among these synthetic polymers, poly(3-hydroxybutyrate-co-3-hydroxyvalerate) (PHBV) microbial polyester can be noted as a biocompatible and biodegradable copolymer. PHBV is a material with suitable properties for cellular growth and adhesion with controllable degradation.[20–30] *In vivo* experiments with oriented matrices have a higher growth value than isotropic matrices of the same material. Various cells recognize a 3D geometrical structure on the surface of substrates, and their growth can be guided and controlled by fabricating microgrooves on substrate surfaces. The cells exhibit sensitivity to the dimensions of the microgrooves. Most of the microgrooves have been fabricated on inorganic substrates, such as micromachined silicon chips which are not very desirable for implantation. Micropatterned regions on glass coverslips with adsorbed laminin have been demonstrated to provide chemical guidance for axonal outgrowth.[31,32]

In this study, oriented PHBV conduit was fabricated by micropatterned wafers. The polymeric conduit was evaluated by scanning electron microscope (SEM), physical and mechanical analyses, and cell culture assay. The designed conduit was filled with SCs and then was implanted into a 30 mm gap in the sciatic nerves of rats. Regenerated nerves were investigated by the histological and behavioral analyses, 4 months after surgery.

Materials and Methods

Design of Oriented Porous Scaffold

PHBV was purchased from Sigma-Aldrich (St. Louis, MO) and 2,2,2-trifluoroethanol used to prepare PHBV solution was also purchased from Sigma-Aldrich and used as received, without further purification. Quartz substrates were etched using reactive ion etching through the mask, leaving behind long rectangular areas capped by chrome. Reactive ion etching is a dry developed process with an etch rate of about 30 nm/min and a resolution of 2 μm. After the chrome was removed from the quartz substrate, the quartz substrates were used as a micro dye for transferring the geometric microgrooves to the biodegradable polymer. Films were produced by casting solutions of PHBV in chloroform, and then polyvinyl alcohol (10%, w/v) was added to this solution to serve as a porogen. Designed solution spin

From the *Proteomics Research Center, Faculty of Paramedical Sciences, Shahid Beheshti University of Medical Sciences, Tehran, Iran; †Department of Biomedical Engineering, Tonekabon Branch, Islamic Azad University, Tonekabon, Iran; ‡Neuroscience Research Center, Shahid Beheshti University of Medical Sciences, Tehran, Iran; §Department of Biomaterials, Faculty of Biomedical Engineering, Science and Research Branch, Islamic Azad University, Tehran, Iran.

Submitted for consideration October 2013; accepted for publication in revised form November 2013.

Disclosure: The authors have no conflicts of interest to report.

Reprint Requests: Esmaeil Biazar, Islamic Azad University, Tonekabon, Iran. Email: kia_esm@yahoo.com.

DOI: 10.1097/MAT.0000000000000044

casting them onto the micropatterned silicon wafers. The PHBV solution was spun on the substrate at 1,800 rpm for 1 minute. After drying for 24 hours, the films were floated off the silicon wafers onto the surface of water and used. The films were then repeatedly washed in distilled water to extract polyvinyl alcohol because it was soluble in water whereas the others were not, and thus a porous micropatterned film was obtained. We used a microwave plasma source to modify the surface of the scaffolds. The microwave plasma has significant advantage over other techniques like radio frequency glow discharge, frequently used in polymer surface modifications. Microwave sources could be operated at low pressures (10^{-3} to 10^{-1} mbar), which reduced the risk of gas phase contamination during processing. Moreover, the plasma properties could be controlled conveniently by adjusting the microwave power. Hence, the surface modification of this polymer became important. In previous article, we modified the surface of scaffolds with oxygen plasma at 60 seconds.[23] The irradiated samples were investigated by physical and mechanical analyses and microscopic and cellular investigations. The plasma surface treatment was reached in the microwave-induced plasma with a surface wave at the power level of 100 W. The experimental setup has been shown in **Figure 1**.

Preparation of 3D Nerve Conduit

The surface characteristics of scaffolds were investigated by an SEM (Cambridge Stereo-scan, S-360; Wetzlar, Germany). The samples were first gold-sputtered for 2 hours (Ion Sputter, JFC-1100; JOEL, Tokyo, Japan) to provide surface conduction before scanning. The sample surfaces static contact angles were investigated by a contact angle measuring apparatus (Krüss G10, Matthews, NC) according to the sessile drop method. For mechanical investigations, the neural guides were subjected to stress–strain analysis using a universal testing machine under an extension rate of 5 mm/min and 100 N load cell. The specific surface area of guides was determined by the surface area and pore size analyzer (BEL Japan, Tokyo, Japan). The oriented film (**Figure 2A**) (33 mm in length and 5 mm in width) was rolled around the cylindrical rod to form a 3D tubular structure and was maintained in this form using a thermal agent (**Figure 2B**).

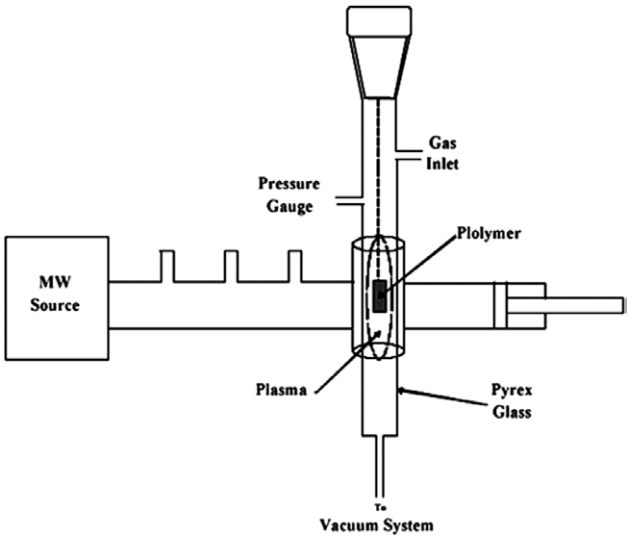

Figure 1. Experimental setup of microwave plasma.

Cell Culture

Schwann cells were obtained from sciatic nerves of 8-day-old rats according to earlier described methods.[33] In brief, the nerve segments were washed in Dulbecco's modified Eagle's medium (DMEM)/F-12 twice and then resuspended in 0.3% collagenase type II solution (100 µl per segment) and incubated for 30 minutes at 37°C. After incubation, the enzymatic solution was carefully removed, and an equal volume of 0.25% trypsin-ethylene diamine tetra-acetic acid (EDTA) was added. The nerve segments were incubated for another 5 minutes at 37°C and then mechanically dissociated until they formed a homogeneous suspension. The SC basal medium was then added to the suspension at a ratio of 4:1 to terminate the activity of the trypsin. The mixture was centrifuged at 800–1,000 rpm for 5 minutes. The supernatant was discarded, and the cells were resuspended in SC basal medium. The SCs were proliferated in the flask, and for subculturing, the SCs were washed using phosphate-buffered saline (PBS). Then the trypsin enzyme/EDTA was added to the flask (37°C), and the flask was incubated for 90 seconds. The culture media (fetal bovine serum/DMEM) was added to the flask, and the cells were gently pipetted. Then the cell suspension was transferred to a tube (15 ml) (BD Falcon; Bioscience, San Jose, CA) and centrifuged (400*g*) (Eppendorf International 5702 model, Hamburg, Germany) for 5 minutes. The solution was removed, and the precipitation was transferred to a new flask (75 cm) for reculturing. Pieces of cell culture (1 cm ×1 cm) from the petri dish (Control) and the main sample were placed individually in one of the Petri dish wells by using a sterilized pincer. A total of 200,000 cells/well were seeded into a 24 well culture plate and then removed by a pipette and poured onto the control and the main samples. For scanning electron microscopy study, the cultured neural guides with SCs were washed by PBS and then fixed by glutaraldehyde (2.5%) at 4°C for 2 hours. The samples were dehydrated by alcohols and then kept with tetroxide osmium vapors at 4°C for 2 hours. The samples were kept in a desiccator, then coated with gold, and investigated by an SEM (Cambridge Stereo-scan, S-360).

Animals and Surgical Procedure

From 20 male Wistar white rats aged approximately 4–8 weeks at the beginning of the experiment and weighing 180–220 g, five defects each were grafted with polymeric conduit without SCs (group A), five defects each were grafted with conduit filled with SC (6×10^6) (group B), five defects each were grafted with autograft group as the positive control (group C), and five defects with nongrafted group as the negative control (group D). The entire experimental protocol was approved by the Institutional Animal Care and Use Committee of Shahid Beheshti University of Medical Sciences, Iran. Animals were handled according to the guidelines established for animal care at the center. A long segment of sciatic nerve was resected, leaving a 30 mm gap caused by retraction of nerve endings. In the autograft group, a 30 mm segment of sciatic nerve was excised, reversed, and sutured back in place. Polymeric tubes of 33 mm in length were used so that the two nerve ends could be slided for 15 mm into the tube and anchored with two epiperineural sutures. A 30 mm gap was thus maintained between the nerve stumps inside the tube. After surgery, the animals were placed in separate cages. All animals had free access to standard rat food and water.

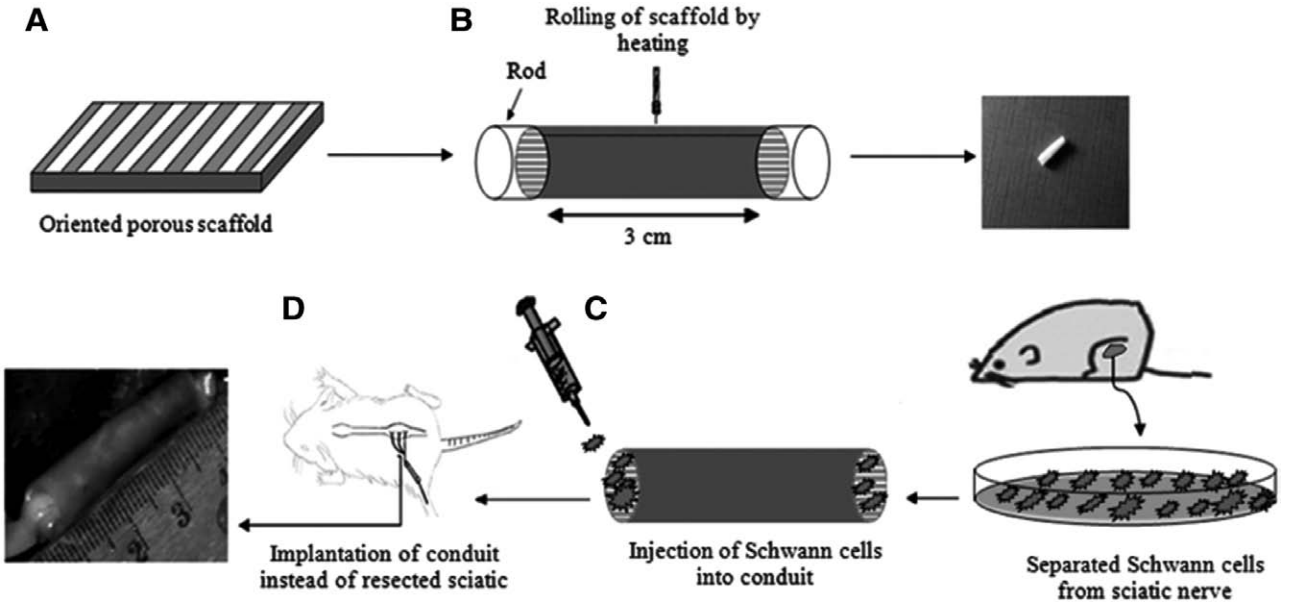

Figure 2. The grafting process of conduit in resected sciatic nerve segment. The oriented film fabricated by micropatterned wafers (**A**), the tube formation by rolling of film by heat sealing process (**B**), injection of Schwann cells into conduit (**C**), and implantation of artificial nerve graft instead of resected sciatic nerve segment (**D**).

Macroscopic Analysis

At 4 months after surgery, the rats were sacrificed, and the regenerated nerves in the control, autograft, and polymeric groups were resected for macroscopic analysis.

Histological and Morphological Studies

For histological analysis, rat middle sciatic nerve cords were removed and fixed in 10% formalin at 4°C for 5 days, dehydrated, and then paraffin embedded. Serial 2 μm paraffin sections were cut with a Senior Precision Rotary Microtome (Model-RMT-30, Haryana, India), stained with toluidine blue (Sigma-Aldrich) according to routine histology protocol, and examined by an optical microscope (Carl Zeiss, Oberkochen, Germany). Myelin thickness was calculated based on Image J software (version 1.41; National Institutes of Health, Rockville, MD). The gastrocnemius muscles were harvested from the operated limbs of rats in all groups, fixed in 5% glutaraldehyde aqueous solution, and then cut into 10 μm thick sections. Then the sections were stained by Masson's trichrome staining and observed under the optical microscope (Nikon Instrument Inc., NY). The average diameter of the muscle fibers was analyzed using the image analysis system (Image J software, version 1.41; National Institutes of Health).

Behavioral Analyses

Toe-Out Angle

The toe-out angle (TOA) is the angle in degrees between the direction of progression and a reference line, which is defined anatomically from the calcaneus to the tip of the third digit. To determine TOA, the rats were placed into acrylic glass containers (100 cm × 15 cm) with a mirror below it. A camera (Nikon) was positioned underneath the transparent base plate to photograph the plantar surface of the animal's paws. Angles were measured and recorded.[34]

Toe Spreading

For the determination of toe spread (TS), the rats were placed into acrylic glass containers (20 cm × 12 cm × 9 cm) on a transparent base plate and then a camera (Nikon) was positioned underneath the plate to photograph the plantar surface of the

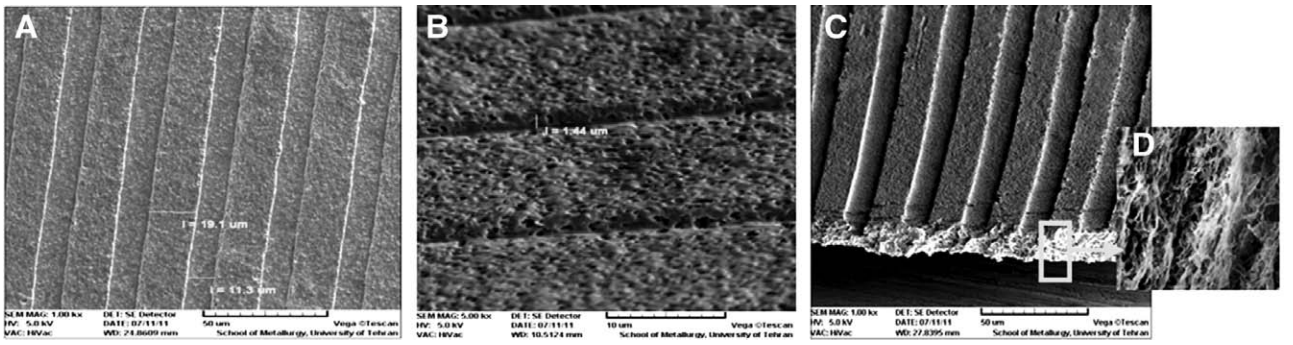

Figure 3. Scanning electron microscope images of the oriented porous poly(3-hydroxybutyrate-co-3-hydroxyvalerate) scaffolds in different magnifications. **A**: 2,000×. **B**: 5,000×. **C**: 1,000×. **D**: 2,000×.

animal's paws. Toe spread factors were determined by measuring the distance between the first and fifth toes (1–5, TS) and between the second and fourth toes (2–4, intermediate TS) as previously described by Bervar.[35]

Toe Spread Factor = [Operated side TS – Nonoperated side TS (NTS)]/NTS; Intermediate TS Factor = [Operated side Intermediate TS – Nonoperated side Intermediate TS (NITS)]/NITS.

Walking Track Analysis

Deficits in descending fine motor control were quantified using walking track or footprint analysis. Footprints were evaluated by three parameters: 1) distance from the heel to the third toe, print length; 2) distance from the first to the fifth toes, TS; and 3) distance from the second to the fourth toes, intermediary TS. All three measurements were taken from the experimental (E) and normal (N) sides. Functional recovery was assessed by calculating the Sciatic Functional Index (SFI) value.[36] SFI = −38.3 [(EPL − NPL)/NPL] + 109.5 [(ETS − NTS)/NTS] + 13.3[(EIT − NIT)/NIT] − 8.8 based on analysis of walking tracks[37] (where EPL = experimental print length, NPL = normal print length, and ETS = experimental toe spread). Postoperatively, the rats were assessed once per month within 4 months after surgery. The investigators were blinded to the animal groups during walking track analysis. SFI 0 and 100 indicate normal function and complete dysfunction, respectively.

Extensor Postural Thrust

All rats were evaluated in 4 months by extensor postural thrust (EPT) analysis. For this test, the entire body of the rat, except the hind limbs, was wrapped in a surgical towel. The foot extensors or force were measured by a digital balance (DE 12K1N model; KERN Co., Germany). As the animal was lowered to the platform, it extended the hindlimbs, anticipating the contact made by the distal metatarsus and digits. The force in grams applied to the digital platform balance (DE 12K1N model; KERN Co.) was recorded. The motor deficit difference between normal and experimental feet was calculated as follows, as described by Koka and Hadlock[38] in 2001:

$$\text{Motor deficit}: \ (\text{NEPT} - \text{EEPT}) / \text{NEPT} \times 100\%$$

where NEPT is normal (unaffected limb) EPT and EEPT is experimental EPT values.

Evaluation of Nociceptive Function

For evaluation of regenerated sensory nerves, the rats were wrapped in a surgical towel above their waist and then positioned to stand with the affected hind paw on a hot water bath at 50°C, and the legs were inserted into the warm water to contact the bottom of the hot water tank. Nociceptive withdrawal reflex was defined as the time elapsed from the onset of hot warm contact to withdrawal of the hind paw and was measured with a stopwatch (Stopwatches Model, Mainland, China).[39]

Statistics Analysis

Data were expressed as mean ± standard deviation. All data were analyzed by one-way analysis of variance with Duncan's multiple range tests ($p < 0.05$ and 0.01; SPSS 16, IBM, Chicago, IL).

Table 1. Mechanical and Physical Properties of Designed Poly(3-hydroxybutyrate-co-3-hydroxyvalerate) Neural Guides

Sample	Porosity (%)	Microgrooved Film Dimensions (Grooved Depth, Widths, Height)	Pore Size	Ultimate Tensile Stress (MPa)
Neural conduit	59 ± 3.2	10/20/2 μm	2 μm	1.9 ± 0.5

The data are presented as mean values ± standard deviation, $p < 0.05$.

Results and Discussion

Characterizations of Polymeric Guide

Figure 3 shows morphology of designed surfaces. **Figure 3A** shows oriented microgrooved surface with dimensions of about 10/20/2 μm, this is suitable for axon movement and nerve regeneration within the construct. In the SEM image in **Figure 3B**, the maximum pore size observed on the patterned film is around 2 μm, and therefore, it is smaller than the size of most neural cells. Similarly, a 1–10 μm pore size was reported in the construction of nerve guides.[40] Thus, this level of pore size on the micropatterned film would allow the nutrients to permeate, however, would not allow the permeation of the cells forcing the cells to remain in the tube, align, and migrate along the axis of the micropatterns. **Figure 3**, **C** and **D** shows SEM images of the microgrooved PHBV film and cross section of surface with its porous structure. The porosity was determined as 59% ± 3.2%. Mechanical and physical properties of designed PHBV sample are shown in **Tables 1** and **2**. **Table 2** shows effect of surface modification of designed sample by oxygen plasma radiation. Plasma-modified PHBV film has lower contact angle compared with unmodified film; therefore, plasma-modified film shows better hydrophilicity that can be suitable for cell attachment.

Cell Culture Results

Figure 4 shows the attached cells on the unmodified and modified PHBV neural guides and the control ones. Cellular images show a good cell growth in the vicinity of PHBV neural guide modified by oxygen plasma. **Figure 5** shows SEM images of cultured SCs in the samples. Figures show high attachment of the SCs on both the surfaces especially for the plasma-modified PHBV neural guide. **Figure 5B** shows well fusiform neural cell with its frills such dendrites.

Table 2. Contact Angle Analysis of Designed Poly(3-hydroxybutyrate-co-3-hydroxyvalerate) Neural Guides

T (°C)	Unmodified Neural Conduit	Plasma-Modified Neural Conduit
Contact angle (deg θ)	107° ± 2.2°	48° ± 2.4°

Data are presented as mean values ± standard deviation, $p < 0.05$.

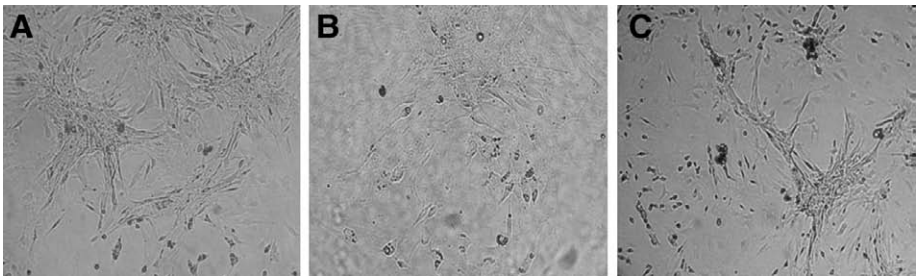

Figure 4. Cell culture on the neural guides and the control. The control (tissue culture polystyrene; TCPS) (**A**), the unmodified neural guide (**B**), and the modified neural guide (**C**).

Macroscopic Results

Figure 6 shows the regenerated sciatic nerve at 4 months after surgery. Reconstructed nerves were not observed in the control group, but sciatic nerve regeneration and neural cord formation were observed in the autograft, polymeric conduit without SCs, and with cells groups. In the autograft group (B), regenerated sciatic nerve shows uniform shape and its size is proportional to the extent of complementarity between proximal and distal ends. In the polymeric film conduit group without SCs (C), sciatic nerve shows unsuitable formation of neural cord. In the polymeric film conduit group with SC group (D), neural cord was formed but was not proportional, with uniform and less thick appearance in the middle and distal parts.

Histological Results

Microscopic images of the middle section of stained sciatic nerve with toluidine blue are shown in **Figure 7**. At 4 months after surgery, suitable regenerated nerve fibers with myelin sheet were observed in the autograft group, and myelinated nerve fibers were formed in the polymeric conduit groups with SCs but were not observed in the polymeric conduit group without cells. The myelin sheath thickness in the polymeric conduit without cell, polymeric conduit with cell, and autograft groups was 0.55 ± 0.01, 0.81 ± 0.06, and 0.85 ± 0.04 μm, respectively. The average myelin sheath thickness in the polymeric conduit with cell group was similar to that in the autograft group ($p < 0.05$).

Polymeric conduits with SC conduits can increase the expression of S-100 and glial fibrillary acidic protein (GFAP), cellular markers of SCs, and glial cells in injured nerve tissue. **Figure 8** shows the expression of S-100 and GFAP in the sciatic nerve samples harvested from the autograft and polymeric film conduit.

Results of Behavioral Analyses

Toe-Out Angle Analysis

Angle between normal and experimental feet calculated by TOA analysis is shown in **Figure 9**. At 4 months after surgery, TOA of the normal foot was significantly less than that of the experimental foot in each group (**Table 3**). The autograft and polymeric film conduit with cell groups showed a better neurofunctional recovery than the control group ($p < 0.01$, $p < 0.05$). The neurofunctional recovery was similar between autograft and polymeric film conduit with cell groups.

Toe Spreading

Toe spread was analyzed by measuring the TS factor and the intermediate TS factor of the left (contralateral to the lesion site) and right (ipsilateral to the lesion site) paws of animals. At 4 months after surgery, the control group showed loss of TS. During the observation period, rat TS improved significantly in the autograft and polymeric conduit groups with cells compared with the control group ($p < 0.01$, 0.05; **Table 4**), but there was no significant difference in TS between autograft and conduit groups with cells groups ($p > 0.05$; **Table 4**).

Walking Track Analysis

Neurofunctional recovery was assessed by walking track analysis, and SFI was obtained. At 4 months after surgery, SFI was 40.1 ± 1.3, 58.2 ± 1.4, 41.4 ± 1.1, and 91.1 ± 1.8 in the autograft, polymeric conduit groups without cells, with cells and control groups, respectively. SFI analyses showed that neurofunctional recovery was better in the autograft and conduit groups with cells groups than in the other groups ($p < 0.05$).

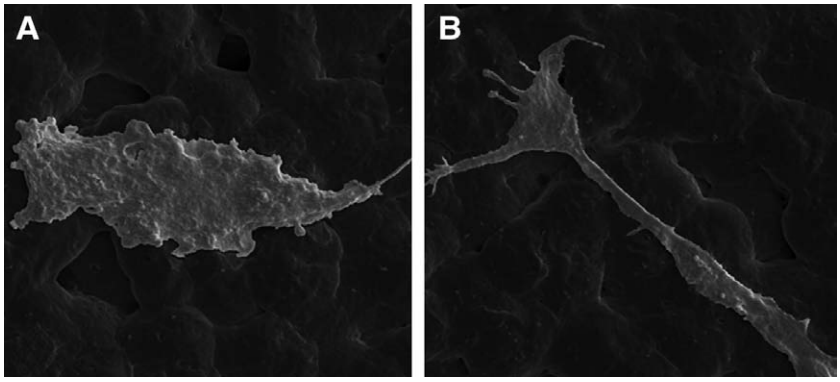

Figure 5. Scanning electron microscope images of cultured Schwann cells on the neural guides. The unmodified poly(3-hydroxybutyrate-co-3-hydroxyvalerate) (PHBV) neural guide (**A**) and the plasma-modified PHBV neural guide (**B**) (2,000×).

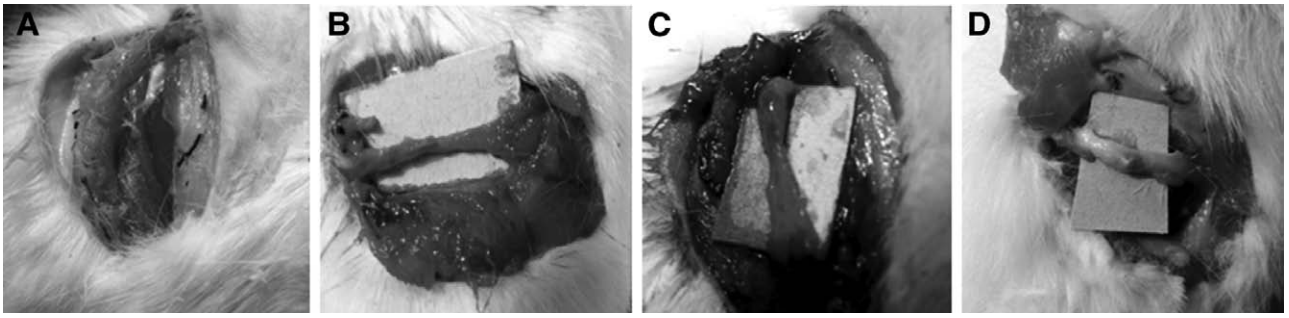

Figure 6. Regenerated section of the sciatic nerve at 4 months after surgery. The control (**A**), the autograft (**B**), the plasma-modified conduit without Schwann cells (**C**), and the plasma-modified conduit with Schwann cells (**D**).

Extensor Postural Thrust Analysis

At 1 month after surgery, the extensor postural trust was similar and high in the polymeric conduit and autograft groups (about 85% and 100%) **(Figure 10)**. The extensor postural trust was recovered significantly in the following months except in the control group. At 4 months after surgery, motor deficits were decreased to about 45% and 40% in the polymeric conduit with SCs and autograft groups, respectively.

Nociceptive Function

Nociceptive function was assessed by withdrawal reflex latency (WRL) analysis. At 1 month after surgery, latency was similar to and high in the polymeric conduits and autograft groups (7–12 seconds). In the following months, nociceptive function significantly recovered in both the polymeric conduits and autograft groups. At the end of the fourth month, nociceptive function recovered more obviously in both polymeric conduit with SC and autograft groups compared with the others group ($p < 0.01$ or $p < 0.05$). However, the control group rats still presented severe loss of nociceptive function at 4 months after surgery (**Figure 11**).

The results showed that when the conduits filled with SCs were implanted into the nerve gaps, recovered motor and nociception functional after 4 months of surgery. The plasma-modified PHBV conduits have several advantages such as biocompatibility, biodegradability, mechanical and physical properties especially its piezoelectric property that can be fabricated electric signal by environment pressure.[20] They can be bent to an angle of up to 180° and brought back to their original shape, an ability that is necessary for adaptation inside a living system. Moreover, they have a thin wall and a highly porous structure, which are important determinants for nutrient transport into the conduit.[41–44] A further advantage of this type of conduit is that it can be easily fabricated and rolled to any required length and diameter with heating process. These properties make PHBV conduits highly suitable for use in artificial nerve scaffolds.[45]

The studies were conducted on the application of artificial neural tube to form neural cords.[46–48] Clinical investigations showed functional improvement and regeneration of peripheral nerve tissue with a gap of 3–5 mm by silicone tube.[49] One of the scaffolds for nerve regeneration was polyglycolic acid (PGA) tubes that were successful for rebuilding of neural fibers.[50,51] Researchers examined nerve regeneration across a long gap in the dog peroneal nerve using a novel artificial nerve conduit (PGA collagen tube). The nerve conduits were implanted across large gaps in the cat[50] and dog[51] nerves. Microscopic observations of the regenerated nerve segments showed numerous myelinated nerve fibers, which were smaller in diameter and enclosed in a thinner myelin sheath than normal axons. These results suggested that artificial nerve conduit has potential usefulness in enhancing peripheral nerve regeneration even across large gaps. Researchers found that the SCs improved peripheral nerve regeneration as assessed using histology, electrophysiology, and behavioral analysis.[52] As shown by Williams *et al.*,[53] SCs may have an impact on peripheral nerve regeneration in the early phases. Bryan *et al.*[54] investigated this early impact by bridging a 20 mm, a fairly long, nerve gap in a rat model by using a poly-L-lysine precoated polyethylene guide filled with preestablished SCs. Cell-seeded guides had better results in axon counts and nerve conduction velocity. The positive impact of SCs on the

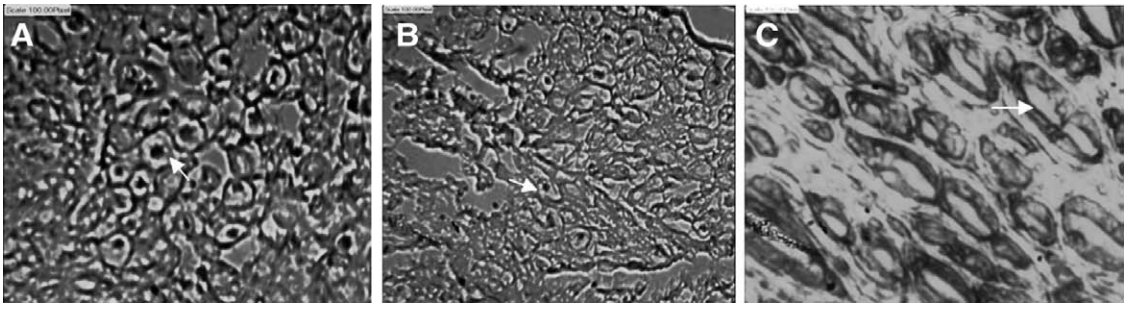

Figure 7. Light micrograph of middle section of the sciatic nerve cable grown between the gaps of 30 mm at 4 months after surgery. The autograft (**A**), the plasma-modified conduit without Schwann cells (**B**), and the plasma-modified conduit with Schwann cells (**C**). Arrows indicate the myelinated nerve. Scale bars: 5 μm.

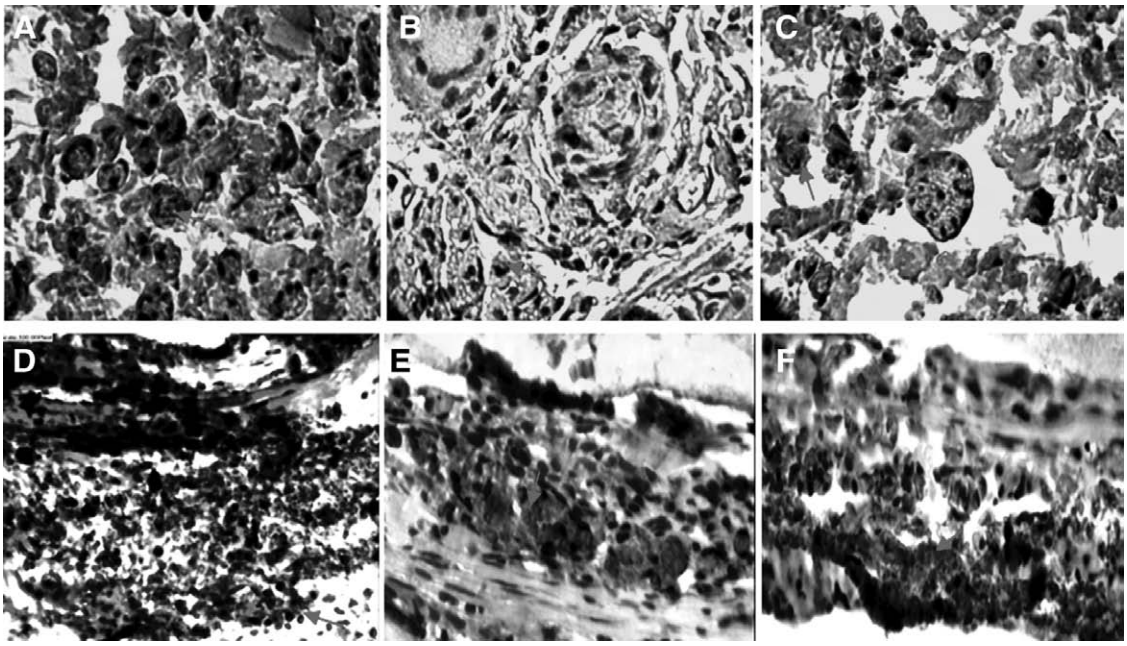

Figure 8. Stained images of sciatic nerve samples expressing cellular markers S-100 (**A**–**C**) and glial fibrillary acidic protein (GFAP; **D**–**F**) harvested from autograft (A and D), polymeric film conduit without cell (B and E), and polymeric film conduit with cell groups (C and F). Arrows indicate S-100-positive Schwann cells and GFAP-positive glial cells, respectively (scale bar: 10 μm for S-100 and scale bars: 20 μm for GFAP).

repair process might be because of the directing cue that SCs provided. Rodriguez *et al*.[55] investigated the influence of syngeneic (genetically identical), isogeneic (genetically alike), and autologous SCs on peripheral nerve regeneration using a mouse model. The regeneration process aided by autologous SC-seeded conduit showed the best result and was similar to the one with an autologous nerve graft. Isogeneic SC-seeded guides gave a lower recovery result, while

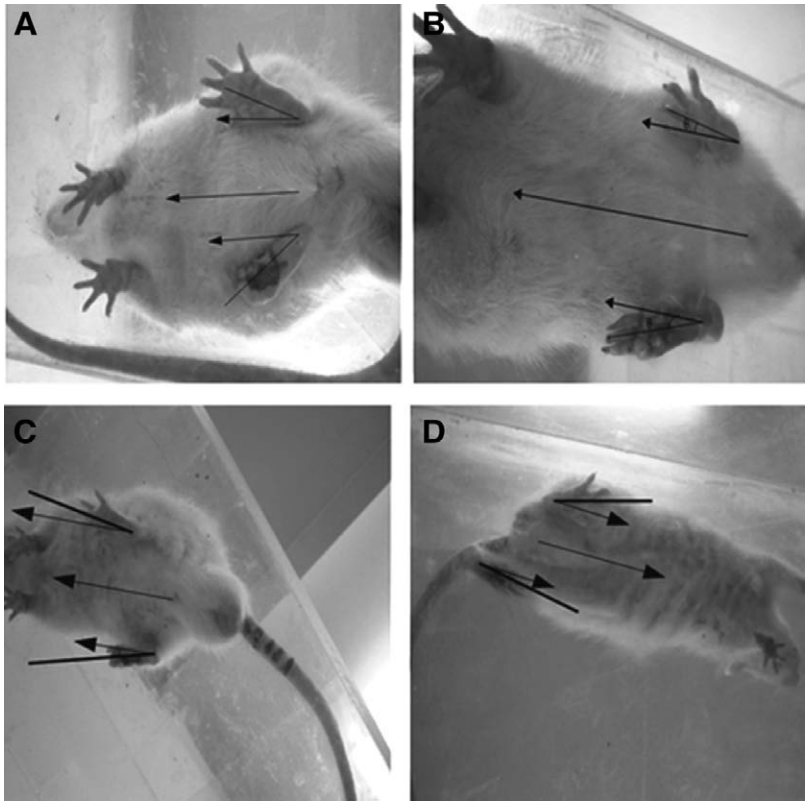

Figure 9. The angle among two feet of normal and experimental for the grafted samples with the control (**A**), autograft (**B**), the plasma-modified conduit without Schwann cells (**C**), and the plasma-modified conduit with Schwann cells (**D**).

Table 3. Toe-Out Angle in Rats with Sciatic Nerve Defect in Each Group

Foot (Degree)	Polymeric Conduit Without Schwann Cells	Polymeric Conduit With Schwann Cells	Autograft	Control
Normal	10 ± 0.3	13 ± 0.9	12 ± 0.4	17 ± 0.6
Experimental	21 ± 0.2*	18 ± 0.5†	19 ± 0.6†	40 ± 0.8*

Data are expressed as mean ± standard deviation from five rats per group.
*$p < 0.05$,
†$p < 0.01$, *vs*. control group.

Table 4. Toe Spread Factors in Rats With Sciatic Nerve Defect in Each Group

Index	Polymeric Conduit Without Schwann Cells	Polymeric Conduit With Schwann Cells	Autograft	Control
Toe spread factor	–0.5 ± 0.02	–0.3 ± 0.08	–0.4 ± 0.04	–0.7 ± 0.09
Intermediate toe spread factor	–0.4 ± 0.01*	–0.2 ± 0.05†	–0.2 ± 0.01†	–0.8 ± 0.03

Toe spread factor = [Operated side toe spread – NTS]/NTS. Intermediate toe spread factor = [Operated side intermediate toe spread – NITS]/NITS. Data are expressed as mean ± standard deviation from five rats per group.
*$p < 0.05$,
†$p < 0.01$, *vs*. control group.
NTS, nonoperated side toe spread; NITS, nonoperated side intermediate toe spread.

syngeneic SCs did not seem to enhance the regeneration process. Lohmeyer *et al*.[56] filled a collagen conduit with polyglactin (a synthetic absorbable polyester commonly used as suturing material) filaments seeded with SCs and isogeneic SCs suspended in Matrigel and used it to repair a 20 mm sciatic nerve gap in a rat model. Although the number of myelinated axons, which crossed the gap to reach the distal stump, was significantly greater in the SC-seeded conduits than those in unseeded ones, the number of regenerated axons was still insufficient to regain the motor function. This might be due to granuloma formation or the foreign body reaction caused by degraded polyglactin filaments, which either physically hindered the regeneration process or adversely affected cell function. In this study, we investigated locomotion and nociception functional for regenerated nerve using oxygen plasma-modified-oriented PHBV conduit and filled with and without SCs in the rat sciatic nerve model. Walking track analysis has frequently been used to reliably determine functional recovery following nerve repair in rat models. SFI obtained was about –41, –58, and –40 for grafted nerves with nerve conduit filled with SCs, conduits without cells, and autograft, respectively.

Results of the comparative functional assessments showed that the difference between the grafted nerves with conduit/SCs and autograft were not significant in terms of motor and nociceptive recovery. The reflex results in EPT analysis is initiated by stretching of the spindles in the interosseous muscles and stimulation of sensory receptors of the foot. A steady recovery of motor deficit occurred throughout the 4 months after surgery in the grafted groups with nerve conduit especially for the conduit/SCs and autograft. Nociception in WRL analysis recovered to a significantly larger extent in the conduits and the autograft groups compared with the control group. At the end of 4 months, mean latency time was good in the grafted groups except the control group. Interestingly, when the nerve is transected and again regenerated, sensory neurons exhibit a faster regenerative pattern than motor neurons. This study again supports

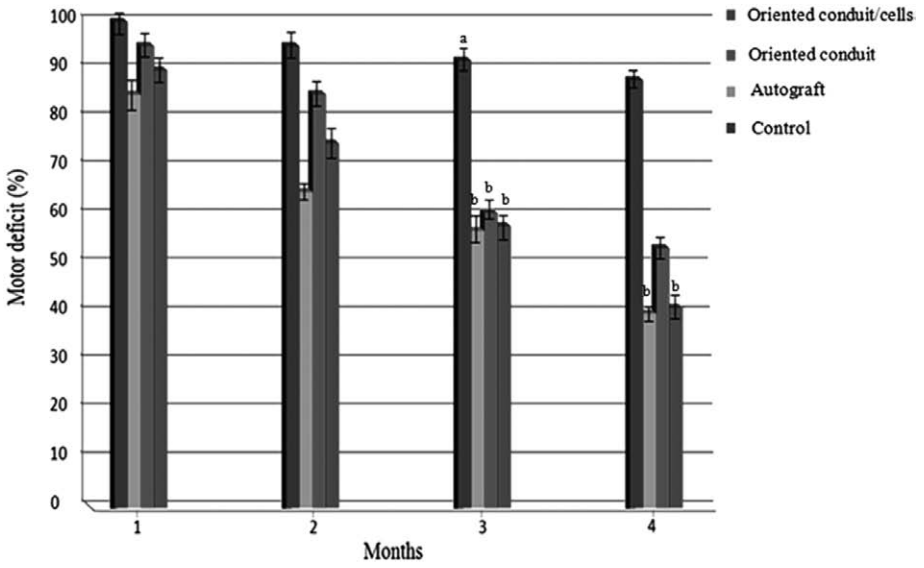

Figure 10. The extensor postural thrust test (percentage of motor deficits) results of rats with sciatic nerve defect in the polymeric conduits and autograft groups at 1–4 months after surgery. Values are expressed as mean ± standard deviation. $^{a}p < 0.05$, $^{b}p < 0.01$, *vs*. control group. n = 5 rats in each group at each time point.

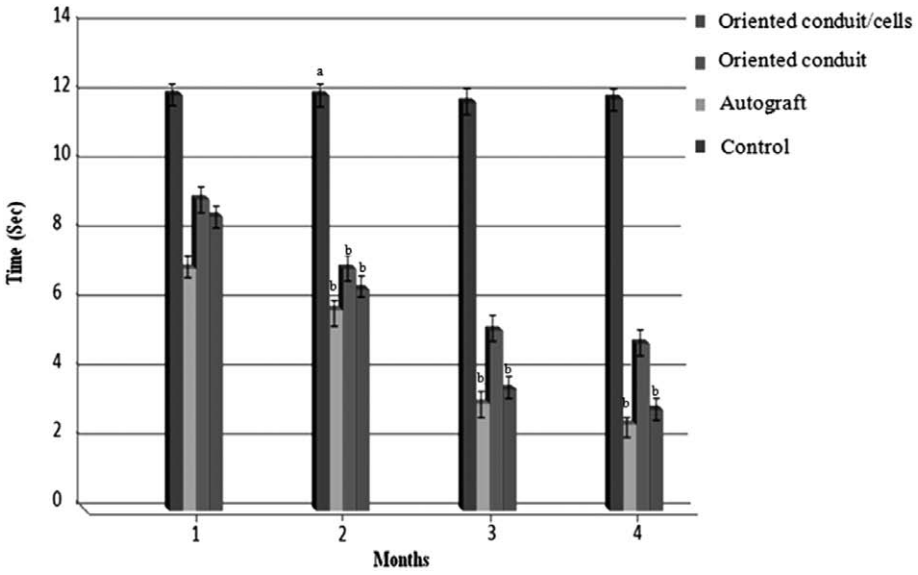

Figure 11. Nociceptive function of rats with sciatic nerve defect in the polymeric conduits and autograft groups by withdrawal reflex latency at 1–4 months after surgery. Values are expressed as mean ± standard deviation. $^{a}p < 0.05$, $^{b}p < 0.01$, *vs*. control group. n = 5 rats in each group at each time point.

the idea that these analyses are more comprehensive than histomorphometrical methods.

Conclusion

In this study, a tubular, oriented, biodegradable, polymeric nerve guidance conduit with SCs was designed for use in the restoration of the function of injured nerve tissues. The oriented porous PHBV nerve conduit was implanted into rat sciatic nerve injury across the 30 mm long defect. The nerve conduits showed suitable structural properties as nerve graft and also SCs well adhered on polymeric surfaces especially on the plasma-modified polymeric surface. At 4 months after surgery, it was observed that the sciatic nerve truck had been reconstructed with restoration of nerve continuity and formation of nerve fibers with myelination. Rats were evaluated by TOA, TS, walking track, EPT, and nociceptive function (WRL) analyses after 4 months of surgery. The grafted samples with conduits showed promising results. Recovery of motor and sensory functions was observed for the conduits and the autograft samples. Accordingly, this study proves the feasibility of the oriented PHBV nerve graft filled with SC for promoting nerve regeneration, raises new possibilities of seeking alternatives to autograft for nerve repair, and establishes an experimental basis for constructing tissue-engineered nerve grafts favorable to an implantation into peripheral nerve with a larger defect. Furthermore, it is possible that this study will allow improvements to meet clinical trial requirements in the future.

References

1. Lee SK, Wolfe SW: Peripheral nerve injury and repair. *J Am Acad Orthop Surg* 8: 243–252, 2000.
2. Burnett MG, Zager EL: Pathophysiology of peripheral nerve injury: A brief review. *Neurosurg Focus* 16: E1, 2004.
3. Yin Q, Kemp GJ, Frostick SP: Neurotrophins, neurones and peripheral nerve regeneration. *J Hand Surg Br* 23: 433–437, 1998.
4. Biazar E, Khorasani MT, Montazeri N, et al: Types of neural guides and using nanotechnology for peripheral nerve reconstruction. *Int J Nanomedicine* 5: 839–852, 2010.
5. Ghaemmaghami F, Behnamfar F, Saberi H: Immediate grafting of transected obturator nerve during radical hysterectomy. *Int J Surg* 7: 168–169, 2009.
6. Firouzi M, Moshayedi P, Saberi H, et al: Transplantation of Schwann cells to subarachnoid space induces repair in contused rat spinal cord. *Neurosci Lett* 402: 66–70, 2006.
7. Ducker TB, Hayes GJ: Peripheral nerve grafts: Experimental studies in the dog and chimpanzee to define homograft limitations. *J Neurosurg* 32: 236–243, 1970.
8. Evans GR: Tissue engineering strategies for nervous system repair. *Prog Brain Res* 128: 349–363, 2000.
9. Heath CA, Rutkowski GE: The development of bioartificial nerve grafts for peripheral-nerve regeneration. *Trends Biotechnol* 16: 163–168, 1998.
10. Brunelli GA, Battiston B, Vigasio A, Brunelli G, Marocolo D: Bridging nerve defects with combined skeletal muscle and vein conduits. *Microsurgery* 14: 247–251, 1993.
11. Tong XJ, Hirai K, Shimada H, et al: Sciatic nerve regeneration navigated by laminin-fibronectin double coated biodegradable collagen grafts in rats. *Brain Res* 663: 155–162, 1994.
12. Fansa H, Schneider W, Wolf G, Keilhoff G: Host responses after acellular muscle basal lamina allografting used as a matrix for tissue engineered nerve grafts1. *Transplantation* 74: 381–387, 2002.
13. Barcelos AS, Rodrigues AC, Silva MD, Padovani CR: Inside-out vein graft and inside-out artery graft in rat sciatic nerve repair. *Microsurgery* 23: 66–71, 2003.
14. Godard CW, de Ruiter MD, Spinner RJ, et al: Nerve tubes for peripheral nerve repair. *Neurosurg Clin N Am* 1: 91–105, 2009.
15. Gámez E, Goto Y, Nagata K, Iwaki T, Sasaki T, Matsuda T: Photofabricated gelatin-based nerve conduits: Nerve tissue regeneration potentials. *Cell Transplant* 13: 549–564, 2004.
16. Jansen K, van der Werff JF, van Wachem PB, Nicolai JP, de Leij LF, van Luyn MJ: A hyaluronan-based nerve guide: In vitro cytotoxicity, subcutaneous tissue reactions, and degradation in the rat. *Biomaterials* 25: 483–489, 2004.
17. Francel PC, Smith KS, Stevens FA, et al: Regeneration of rat sciatic nerve across a LactoSorb bioresorbable conduit with interposed short-segment nerve grafts. *J Neurosurg* 99: 549–554, 2003.
18. Ahmed Z, Underwood S, Brown RA: Nerve guide material made from fibronectin: Assessment of in vitro properties. *Tissue Eng* 9: 219–231, 2003.

19. Meek MF, den Dunnen WFA, Bartels HL, Robinson PH: Long term evaluation peripheral nerve regeneration and functional nerve recovery after reconstruction with a thin-walled biodegradable poly (DL-lactide-co-caprolactone) nerve guide. *Cell Mater* 7: 53–57, 1997.
20. Williams SF, Martin DP, Horowitz DM, Peoples OP: PHA applications: Addressing the price performance issue: I. Tissue engineering. *Int J Biol Macromol* 25: 111–121, 1999.
21. Hromadka M, Collins JB, Reed C, et al: Nanofiber applications for burn care. *J Burn Care Res* 29: 695–703, 2008.
22. Majdi A, Biazar E, Heidari S: Fabrication and comparison of electro-spun PHBV nanofiber and normal film and its cellular study. *Orient J Chem* 27: 523–528, 2011.
23. Rezaei-Tavirani M, Biazar E, Al J, et al: Fabrication of collagen-coated poly (beta-hydroxy butyrate-co-beta-hydroxyvalerate) nanofiber by chemical and physical methods. *Orient J Cem* 27: 385–395, 2011.
24. Ai J, Heidari SK, Ghorbani F, et al: Fabrication of coated-collagen electrospun PHBV nanofiber film by plasma method and its cellular study. *J Nanomater* 2011: 1–8, 2011.
25. Biazar E, Heidari SK, Pouya M, et al: Nanofibrous nerve conduits for repair of 30-mm-long sciatic nerve defects. *Neural Regen Res* 8: 2266–2274, 2013.
26. Zeinali R, Biazar E, Heidari SK, et al: Regeneration of full-thickness skin defects using umbilical cord blood stem cells loaded into modified porous scaffolds. *ASAIO Journal* 60: 106–114, 2014.
27. Biazar E, Keshel SH: The healing effect of stem cells loaded in nanofibrous scaffolds on full thickness skin defects. *J Biomed Nanotechnol* 9: 1471–1482, 2013.
28. Biazar E, Heidari SK: A nanofibrous PHBV tube with Schwann cell as artificial nerve graft contributing to rat sciatic nerve regeneration across a 30-mm defect bridge. *Cell Commun Adhes* 20: 41–49, 2013.
29. Montazeri M, Rashidi N, Biazar E, et al: Compatibility of cardiac muscle cells on coated-gelatin electro-spun polyhydroxybutyrate/valerate nano fibrous film. *Biosci Biotech Res ASIA* 8: 515–521, 2011.
30. Biazar E, Keshel SH: Chitosan-cross-linked nanofibrous PHBV nerve guide for rat sciatic nerve regeneration across a defect bridge. *ASAIO J* 59: 651–659, 2013.
31. Thompson DM, Buettner HM: Schwann cell response to micropatterned laminin surfaces. *Tissue Eng* 7: 247–265, 2001.
32. Brunette DM, Chehroudi B: The effects of the surface topography of micromachined titanium substrata on cell behavior in vitro and in vivo. *J Biomech Eng* 121: 49–57, 1999.
33. Wei Y, Zhou J, Zheng Z, et al: An improved method for isolating Schwann cells from postnatal rat sciatic nerves. *Cell Tissue Res* 337: 361–369, 2009.
34. Artur SP, Cabrita Antonio M, Geuna S, et al: Toe out angle: A functional index for the evaluation of sciatic nerve recovery in the rat model. *Expe Neurol* 183: 695–699, 2003.
35. Bervar M: Video analysis of standing–an alternative footprint analysis to assess functional loss following injury to the rat sciatic nerve. *J Neurosci Methods* 102: 109–116, 2000.
36. Bozkurt A, Deumens R, Scheffel J, et al: CatWalk gait analysis in assessment of functional recovery after sciatic nerve injury. *J Neurosci Methods* 173: 91–98, 2008.
37. Bain JR, Mackinnon SE, Hunter DA: Functional evaluation of complete sciatic, peroneal, and posterior tibial nerve lesions in the rat. *Plast Reconstr Surg* 83: 129–136, 1989.
38. Koka R, Hadlock TA: Quantification of functional recovery following rat sciatic nerve transection. *Exp Neurol* 168: 192–195, 2001.
39. Masters DB, Berde CB, Dutta SK, et al: Prolonged regional nerve blockade by controlled release of local anesthetic from a biodegradable polymer matrix. *Anesthesiology* 79: 340–346, 1993.
40. Vleggeert-Lankamp CL, de Ruiter GC, Wolfs JF, et al: Pores in synthetic nerve conduits are beneficial to regeneration. *J Biomed Mater Res A* 80: 965–982, 2007.
41. Doi Y: *Microbial Polyesters*. New York, VCH publishers, 1990.
42. Sudesh K, Abe H, Doi Y: Synthesis structure and properties of polyhydroxyalkonates: Biological polyesters. *Prog Polym Sci* 25: 1503–1555, 2000.
43. Holland SJ, Jolly AM, Yasin M, Tighe BJ: Polymers for biodegradable medical devices. II. Hydroxybutyrate-hydroxyvalerate copolymers: Hydrolytic degradation studies. *Biomaterials* 8: 289–295, 1987.
44. Yucel D, Kose GT, Hasirci V: Polyester based nerve guidance conduit design. *Biomaterials* 31: 1596–1603, 2010.
45. Young RC, Wiberg M, Terenghi G: Poly-3-hydroxybutyrate (PHB): A resorbable conduit for long-gap repair in peripheral nerves. *Br J Plast Surg* 55: 235–240, 2002.
46. Archibald SJ, Shefner J, Krarup C, Madison RD: Monkey median nerve repaired by nerve graft or collagen nerve guide tube. *J Neurosci* 15(5 Pt 2): 4109–4123, 1995.
47. Fields RD, Le Beau JM, Longo FM, Ellisman MH: Nerve regeneration through artificial tubular implants. *Prog Neurobiol* 33: 87–134, 1989.
48. Keeley R, Atagi T, Sabelman E, et al: Peripheral nerve regeneration across 14-mm gaps: A comparison of autograft and entubulation repair methods in the rat. *J Reconstr Microsurg* 9: 349–358, discussion 359, 1993.
49. Lundborg G, Rosén B, Dahlin L, Danielsen N, Holmberg J: Tubular versus conventional repair of median and ulnar nerves in the human forearm: Early results from a prospective, randomized, clinical study. *J Hand Surg Am* 22: 99–106, 1997.
50. Kiyotani T, Nakamura T, Shimizu Y, Endo K: Experimental study of nerve regeneration in a biodegradable tube made from collagen and polyglycolic acid. *ASAIO J* 41: M657–M661, 1995.
51. Matsumoto K, Ohnishi K, Sekine T, et al: Use of a newly developed artificial nerve conduit to assist peripheral nerve regeneration across a long gap in dogs. *ASAIO J* 46: 415–420, 2000.
52. Bunge RP: The role of the Schwann cell in trophic support and regeneration. *J Neurol* 242: 19–21, 1994.
53. Williams LR, Longo FM, Powell HC, Lundborg G, Varon S: Spatial-temporal progress of peripheral nerve regeneration within a silicone chamber: Parameters for a bioassay. *J Comp Neurol* 218: 460–470, 1983.
54. Bryan DJ, Wang KK, Chakalis-Haley DP: Effect of Schwann cells in the enhancement of peripheral-nerve regeneration. *J Reconstr Microsurg* 12: 439–436, 1996.
55. Rodríguez FJ, Verdú E, Ceballos D, Navarro X: Nerve guides seeded with autologous Schwann cells improve nerve regeneration. *Exp Neurol* 161: 571–584, 2000.
56. Lohmeyer JA, Shen ZL, Walter GF, Berger A: Bridging extended nerve defects with an artificial nerve graft containing Schwann cells preseeded on polyglactin filaments. *Int J Artif Organs* 30: 64–74, 2007.